

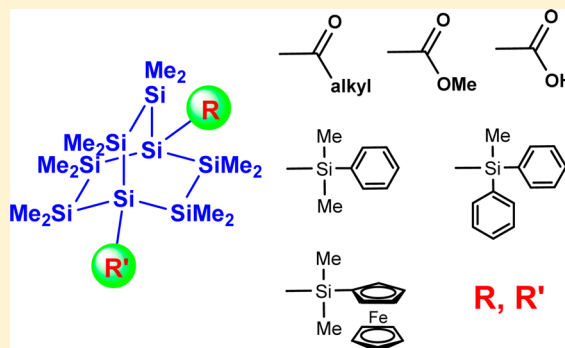
Synthesis and Properties of Bridgehead-Functionalized Permethylbicyclo[2.2.2]octasilanes

Harald Stueger,* Bernd Hasken, Uwe Gross, Roland Fischer, and Ana Torvisco Gomez

Institute of Inorganic Chemistry, Graz University of Technology, Stremayrgasse 9, A-8010 Graz, Austria

Supporting Information

ABSTRACT: A series of previously unknown bridgehead-functionalized bicyclo[2.2.2]octasilanes, $\text{Me}_3\text{Si-Si}_8\text{Me}_{12}\text{-X}$, $\text{X-Si}_8\text{Me}_{12}\text{-X}$, and $\text{X-Si}_8\text{Me}_{12}\text{-Y}$ [X , $\text{Y} = -\text{SiMe}_n\text{Ph}_{3-n}$ ($n = 1, 2$) (2, 3, 10), $-\text{SiMe}_2\text{Fc}$ ($\text{Fc} = \text{ferrocenyl}$) (4, 11, 13, 14), $-\text{COR}$ ($\text{R} = \text{Me}, t\text{Bu}$) (6, 7, 12), COOMe (8), COOH (9)], have been prepared by the reaction of the silanides $\text{Me}_3\text{Si-Si}_8\text{Me}_{12}\text{-K}^+$ or $\text{K}^+\text{-Si}_8\text{Me}_{12}\text{-K}^+$ with proper electrophiles and fully characterized. The molecular structures of 2, 3, 4, 6, 8, 9, 10, and 13 as determined by single-crystal X-ray diffraction analysis exhibit a slightly twisted structure of the bicyclooctasilane cage. Endocyclic bond lengths, bond angles, and dihedral angles are not influenced considerably by the substituents attached to the bridgehead silicon atoms. Due to $\sigma(\text{SiSi})/\pi(\text{aryl})$ conjugation, a 20–30 nm bathochromic shift of the longest wavelength UV absorption band relative to $\text{Me}_3\text{Si-Si}_8\text{Me}_{12}\text{-SiMe}_3$ (1) is evident in the UV absorption spectra of the phenyl and ferrocenyl derivatives. Otherwise, UV absorption data do not support the assumption of aryl/aryl or aryl/C=O interaction via the $\sigma(\text{SiSi})$ bicyclooctasilane framework.



INTRODUCTION

Oligo- and polysilanes have been extensively studied due to their chemical stability and due to their unique electronic properties, which more or less can be related to the extensive delocalization of σ -electrons along the silicon skeleton (σ -delocalization).¹ σ -Delocalization within cyclic Si–Si frameworks is particularly well established,² giving rise to pronounced substituent effects on the properties of the Si–Si backbone such as long-wavelength UV absorption up to the visible range,³ room-temperature photoluminescence,⁴ nonlinear optical behavior,⁵ and photochemical activity.⁶ Furthermore, σ -conjugated cyclopolysilane bridges have been shown to be better mediators for electronic effects in bichromophoric covalently linked donor–bridge–acceptor (D-br-A) compounds as compared to their open-chained counterparts.⁷

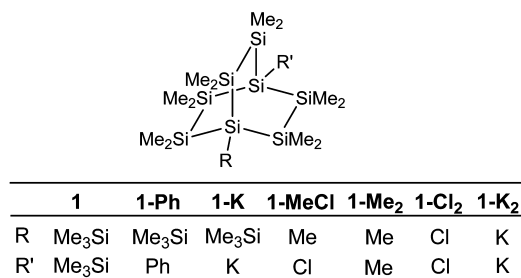
Wurtz-type coupling of diorganodihalosilanes with alkali metals is still the most prominent way for the synthesis of cyclopolysilanes. Due to the harsh reaction conditions, however, this method gives reasonable yields only when simple alkyl or aryl groups are attached to silicon. In order to introduce alternative substituents, the resulting peralkyl- or perarylcyclopolysilanes have to be further functionalized, which is most frequently achieved by selective chlorodemethylation or chlorodephenylation followed by treatment of the resulting organochloropolysilanes with proper nucleophiles. Using this approach a variety of functional groups such as OR, SR, NR_2 , PR_2 , transition metal fragments ML_m , and many others have already been attached to cyclopolysilane backbones with excellent success.⁸

Wurtz-type coupling has also been applied to the synthesis of polysilanes with bicyclic or cage-like structures.⁹ In many cases, however, poor yields and severe problems in the course of the isolation of the desired reaction products were encountered. Thus, tetradecamethylbicyclo[2,2,2]octasilane (**1-Me₂**) has been prepared for the first time in <5% yield by West using Na/K condensation of $\text{Me}_3\text{SiCl}_2/\text{MeSiCl}_3$ mixtures.¹⁰ In order to enhance the selectivity of the coupling reaction Kira et al. reacted two equivalents of $(\text{ClMe}_2\text{Si})_3\text{SiMe}$ with lithium metal and obtained **1-Me₂** in 19% yield.¹¹ Recent achievements in the chemistry of α,ω -oligosilanyldianions mainly by Marschner et al. finally enabled the synthesis of bis(trimethylsilyl)dodecamethylbicyclo[2.2.2]octasilane (**1**) and a whole series of related oligosilane cycles and cages in excellent yields.¹² Furthermore, it has been reported that **1-Me₂** and **1** can be functionalized selectively at the bridgehead Si atoms to give **1-K**, **1-K₂**, **1-MeX**, and **1-X₂** ($\text{X} = \text{Cl}, \text{Br}$) (compare Scheme 1), which represent valuable synthons for further derivatization. In a small-scale experiment Kira et al. obtained **1-Ph** from **1-MeCl** and PhLi in 58% yield.¹³ Nucleophilic substitution reactions of **1-MeCl**, however, turned out to be of limited scope because neither scale-up to preparative amounts nor the synthesis of bicyclo[2.2.2]octasilanes bearing functional aromatic side groups such as p-PhCN or p-PhCF₃ could be accomplished successfully.¹⁴ The reaction of **1-K** and **1-K₂** with various C or Si electrophiles to the corresponding bridgehead-functionalized cages, on the other hand, gave quite satisfactory results.¹⁵

Received: March 6, 2013

Published: August 7, 2013

Scheme 1



For **1-Ph** Kira et al. observed dual fluorescence from the locally excited (LE) and the intramolecular charge transfer (ICT) state even in nonpolar solvents and, thus, were able to demonstrate that bicyclo[2,2,2]octasilane cages can get involved in charge transfer processes.¹³ In contrast to cyclic and open-chained permethyloligosilanes, for which the first visible transition is of $\sigma \rightarrow \sigma^*$ character, TD-DFT calculations published by Marschner and Ottoson recently assigned the longest wavelength UV absorption band in **1** to $\sigma \rightarrow \pi^*$ type electron transitions.¹⁶ The authors of this study further suggest that the electronic structure within bicyclo[2.2.2]octasilane cages may result in charge transport characteristics that are different from those of linear oligosilanes. Therefore, we found it highly desirable to improve the understanding of the impact of various substituent groups on the properties of the Si–Si bond system within the bicyclo[2.2.2]octasilane cage. Herein

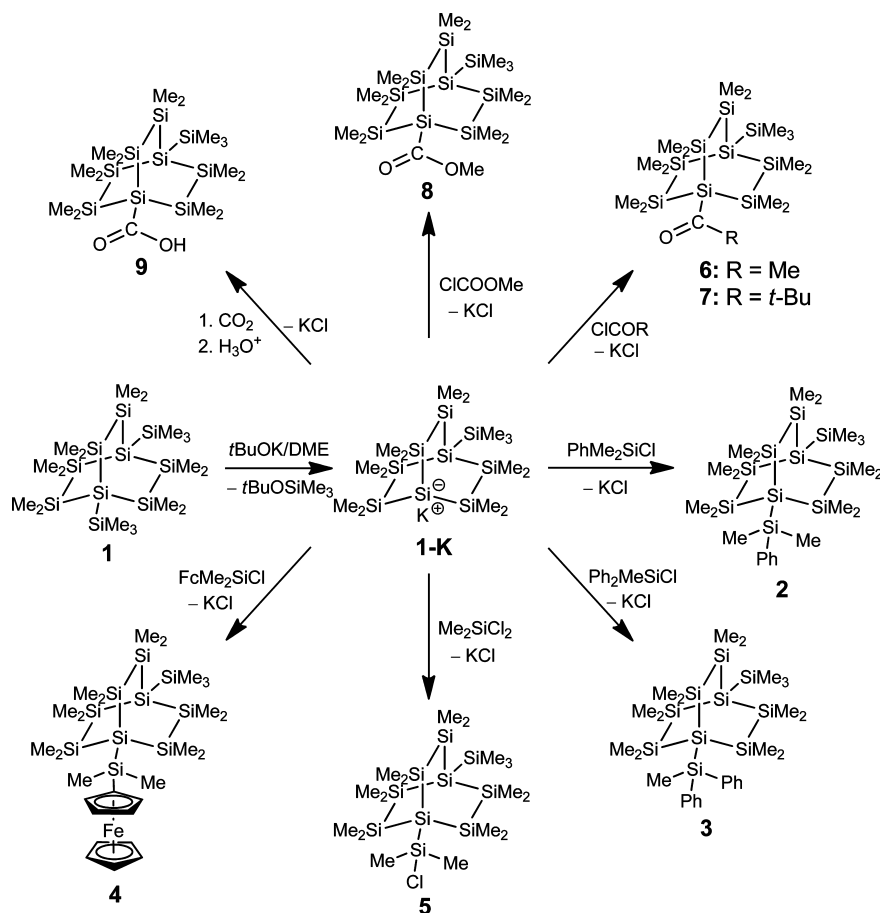
we now would like to report on the synthesis of previously unknown bicyclo[2.2.2]octasilanes with phenyl, ferrocenyl, and carbonyl side groups and on the investigation of substituent effects within the target compounds using mainly UV absorption spectroscopy and X-ray crystallography.

RESULTS AND DISCUSSION

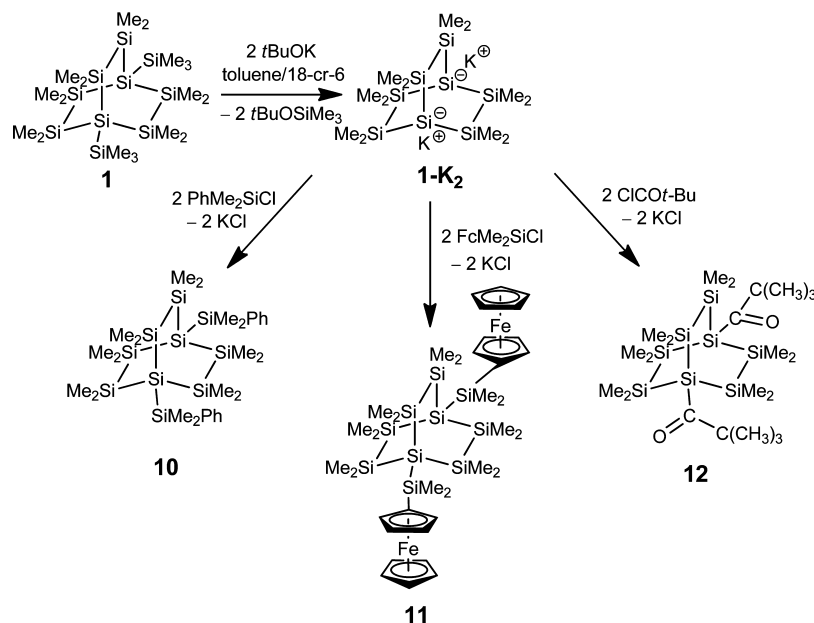
It has been demonstrated earlier that polysilyanyl alkali metal compounds such as $(\text{Me}_3\text{Si})_3\text{SiM}$ ($M = \text{K}, \text{Li}$) smoothly react with various electrophiles to give functional silanes $(\text{Me}_3\text{Si})_3\text{SiX}$ with substituents X such as H, alkyl, SiR_3 , GeR_3 , COR, COOR, or COOH attached to the central silicon atom.¹⁷ In the present study we used a similar approach to synthesize the corresponding bridgehead-functionalized bicyclo[2.2.2]octasilanes **2–12** starting from the potassium silanides **1-K** and **1-K₂**.

As depicted in Scheme 2, **1-K** can easily be silylated with PhMe_2SiCl , Ph_2MeSiCl , or FcMe_2SiCl ($\text{Fc} = \text{ferrocenyl}$) in toluene solution at -70°C to give the air-stable and crystalline compounds **2**, **3**, and **4**, respectively, in yields of $>70\%$. With a 4-fold excess of Me_2SiCl_2 the SiMe_2Cl -substituted product **5** was obtained, which may be used for further derivatization by nucleophilic substitution at the silicon–chlorine bond. Treatment of **1-K** with equimolar amounts of ClCOR ($R = \text{Me}, t\text{Bu}$) or ClCOOMe , furthermore, allowed for the synthesis of the acyl- and methylcarboxybicyclo[2.2.2]octasilanes **6–8**. The corresponding carboxylic acid **9** finally could be obtained by carbonation of **1-K** with CO_2 followed by acid hydrolysis of the

Scheme 2



Scheme 3



primarily formed potassium carboxylate. **6–9** are stable against air and moisture but slowly decompose within several weeks upon storage at room temperature under formation of polymeric products of unidentified composition, which also applies to the acyl and diacyl bicyclo[2.2.2]octasilanes **12** and **14** mentioned below.

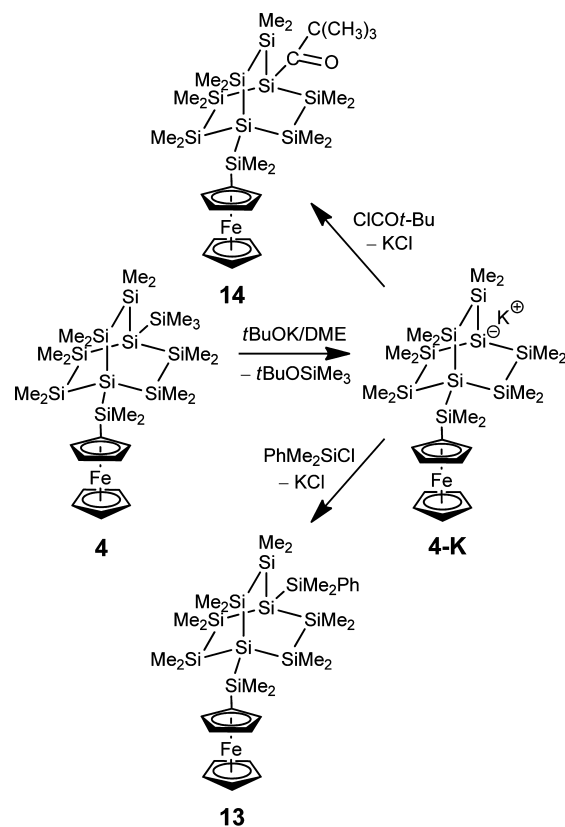
The reaction of **1-K₂** with two equivalents of PhMe₂SiCl, FcMe₂SiCl, or ClCO*t*Bu also proceeded straightforwardly and yielded the symmetrically disubstituted species **10**, **11**, and **12**, respectively (Scheme 3).

If **4** was stirred with a 1.1 molar excess of KO*t*Bu in DME for 40 min at room temperature, the Me₃Si group was split off selectively and the potassium silanide **4-K** was cleanly formed. The ²⁹Si NMR spectrum of the resulting reaction solution exhibits a resonance line at -177.62 ppm, which is easily assigned to the negatively charged bridgehead silicon atom, while the signals of the ≡SiSiMe₃ moiety at -6.11 (SiMe₃) and -130.67 (SiSiMe₃) had disappeared. Subsequent addition of 1.1 equivalents of PhMe₂SiCl or ClCO*t*Bu at -70 °C finally afforded the asymmetrically disubstituted cages **13** and **14** (Scheme 4).

In a similar manner **7** reacted with KO*t*Bu to give the silanide **7-K** with $\delta^{29}\text{Si} = -180.69$ ppm for the silicon atom bearing the negative charge, which could be converted to **12** by addition of another equivalent of ClCO*t*Bu (Scheme 5). The reaction of **8** with KO*t*Bu finally afforded a product mixture of unidentified composition instead of the silanide **8-K**. The ²⁹Si NMR spectra of the resulting reaction solution showed numerous signals that could not be assigned unambiguously.

All previously unknown compounds were fully characterized by spectroscopic means and elemental analyses. Analytical data (compare Experimental Section) are consistent with the proposed structures in all cases. For compounds **3**, **6**, **7** and **12** elemental analyses did not give satisfactory results very likely due to incomplete combustion. In all cases, however, proper HRMS data were obtained. Additionally ¹H- and ²⁹Si NMR spectra of **3**, **6**, **7** and **12** are displayed in the Supporting Information in order to demonstrate the purity of the compounds.

Scheme 4



²⁹Si NMR chemical shift data of the bicyclo[2.2.2]octasilane core are summarized in Table 1. The asymmetrically substituted compounds exhibit two ²⁹Si resonance lines for the SiMe₂ groups, while only one signal appears in the same range of the ²⁹Si spectra of the symmetrical species **10–12**. ²⁹Si chemical shift values near -39 ppm were found for the SiMe₂ groups, which are not significantly influenced by the nature of the substituents X.

Scheme 5

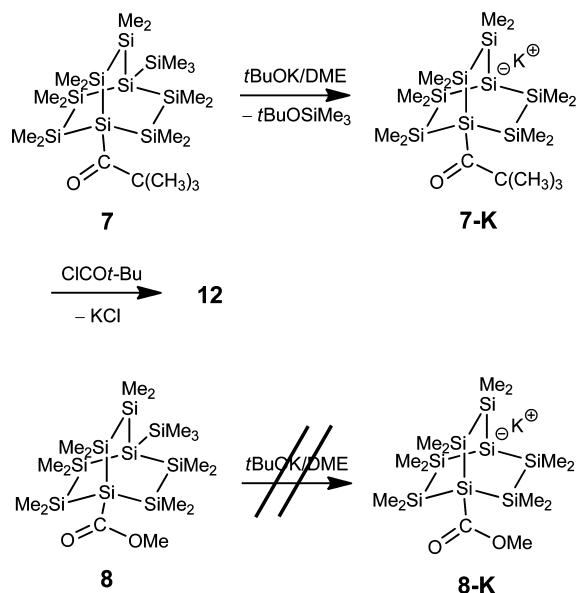


Table 1. $\delta^{29}\text{Si}$ Chemical Shift Data of the Bicyclo[2,2,2]octasilane Core in 1–14 (CDCl_3 solution, vs ext. TMS, ppm)

	SiMe_2	$\equiv\text{SiSiMe}_{3-n}\text{R}_n$	$\equiv\text{SiCOR}'$	$\equiv\text{Si}^{\ominus}\text{K}^{\oplus}$
1 ^a	−38.3	−130.2		
1-K ^b	−33.73; −39.61	−129.57		−178.63
2	−37.89; −38.26	−131.00; −129.04		
3	−37.76; −38.18	−131.45; −128.37		
4	−38.12; −38.31	−130.67; −128.90		
4-K ^b	−34.32; −39.67	−127.89		−177.62
5	−38.21; −38.42	−130.48; −125.01		
6	−38.05; −39.76	−129.78		
7	−37.76; −38.09	−130.82	−75.68	
7-K ^b	−33.05; −40.06		−73.86	−180.69
8	−38.09; −39.19	−129.63	−76.68	
9	−38.12; −39.22	−129.61	−76.72	
10	−37.90	−129.73		
11	−38.14	−129.12		
12	−37.59		−76.88	
13	−37.89; −38.09	−129.28; −129.55		
14	−37.54; −38.10	−129.59	−76.00	

^aTaken from ref 12b. ^bMeasured in DME.

$\delta^{29}\text{Si}$ values for the bridgehead Si atoms close to the ones observed for the corresponding $(\text{Me}_3\text{Si})_3\text{SiX}$ compounds were measured near -130 ppm for the silyl derivatives and -77 ppm for the acyl- and carboxy-substituted species. It is interesting to note that the silanides **1-K**, **4-K**, and **7-K** exhibit a marked low-field shift of the ^{29}Si signal assigned to the tertiary Si atom bearing the negative charge by 15.1–18.2 ppm as compared to $(\text{Me}_3\text{Si})_3\text{SiK}$ ($\delta^{29}\text{Si}$ in DME solution = -195.83 ppm),^{17a} which probably reflects the improved ability for delocalization of the negative charge within the Si–Si framework of the bicyclooctasilane cage. Furthermore, the ^1H NMR spectra feature two SiMe_2 signals for the unsymmetrical species and only one signal for the symmetrical ones, which allows us to conclude that both methyl groups attached to each silicon atom of the bicyclooctasilane moiety are magnetically equivalent due to the symmetric structure of the polysilane cage.

Single crystals suitable for X-ray structure analysis could be grown from compounds **2**, **3**, **4**, **6**, **8**, **9**, **10**, and **13**. The obtained molecular structures are depicted in Figures 1–7 together with selected bond distances, bond angles, and dihedral angles.

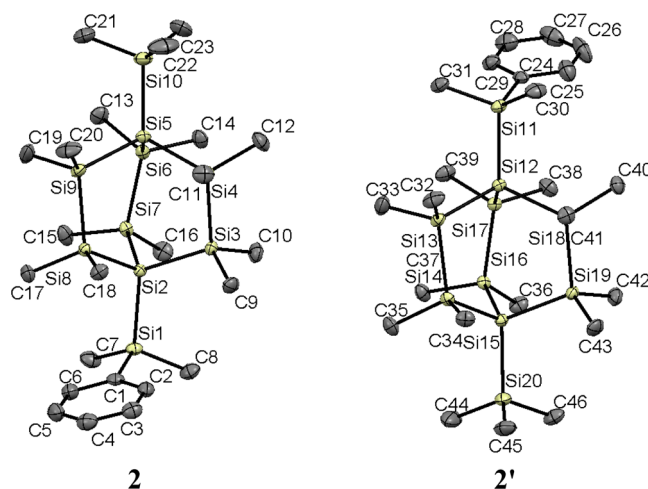


Figure 1. ORTEP diagram for compound **2**. Thermal ellipsoids are depicted at the 50% probability level. Hydrogen atoms are omitted for clarity. The crystals contain two independent molecules (**2**, **2'**) in the asymmetric unit. Selected bond lengths [Å] and bond and torsional angles [deg] with estimated standard deviations: **2**: Si–Si (mean) 2.351, Si(1)–C(1) 1.892(2), Si–C_{methyl} (mean) 1.883, Si–Si–Si (mean) 109.6, C(1)–Si(1)–Si(2) 109.47(5), Si(2)–Si(3)–Si(4)–Si(5) $-18.92(3)$, Si(2)–Si(7)–Si(6)–Si(5) $-18.98(3)$, Si(2)–Si(8)–Si(9)–Si(5) $-18.79(3)$, Si(2)–Si(1)–C(1)–C(2) $-79.0(1)$, Si(2)–Si(1)–C(1)–C(6) 98.8(1). **2'**: Si–Si (mean) 2.351, Si(11)–C(24) 1.884(2), Si–C_{methyl} (mean) 1.884, Si–Si–Si (mean) 109.7, C(24)–Si(11)–Si(12) 109.47(5), Si(15)–Si(16)–Si(17)–Si(12) $-16.32(3)$, Si(15)–Si(14)–Si(13)–Si(12) $-16.24(3)$, Si(12)–Si(18)–Si(19)–Si(15) $-18.40(3)$, Si(12)–Si(11)–C(24)–C(25) $-85.3(1)$, Si(12)–Si(11)–C(24)–C(29) 92.7(1).

The phenyl compounds **2** and **3** crystallize in the triclinic space group $P\bar{1}$ and orthorhombic space group $Pca2(1)$, respectively, with two independent molecules in the asymmetric unit. **2**, **4**, **10**, and **13** exhibit a roughly perpendicular arrangement of the plane of the aromatic rings relative to the adjacent Si–Si bond with torsional angles $\text{C}_{\text{sp}2}\text{–C}_{\text{sp}2}\text{–Si–Si}$ not far from 90° . Deviation from perpendicularity is much larger in compound **3**, which can be ascribed to the steric bulk of the two phenyl rings attached to the same silicon atom. In general a perpendicular geometry is frequently observed within the fragment phenyl–Si–Si because it provides the basis for effective $\sigma(\text{Si–Si})\text{–}\pi(\text{phenyl})$ overlap. A study of the absorption spectra of conformationally constrained arylsilylanes thus demonstrated that a torsion angle between the phenyl ring plane and the Si–Si bond of 90° effects in maximum $\sigma\text{–}\pi$ conjugation.¹⁸ Similar conformational dependence of UV absorption and emission properties was also observed when the 1,2-diphenyldisilane moiety was conformationally constrained by incorporation into cyclic structures.¹⁹

The sum of the bond angles around the carbonyl C atom in **6**, **8**, and **9** is close to 360° and reflects the trigonal planar geometry within the SiRC=O moiety. Carbonyl C=O bond lengths between 1.19 and 1.23 Å were measured, approximately the same as that found in simple organic ketones, carboxylic acids, and esters.²⁰ Silicon carbonyl group bond lengths at

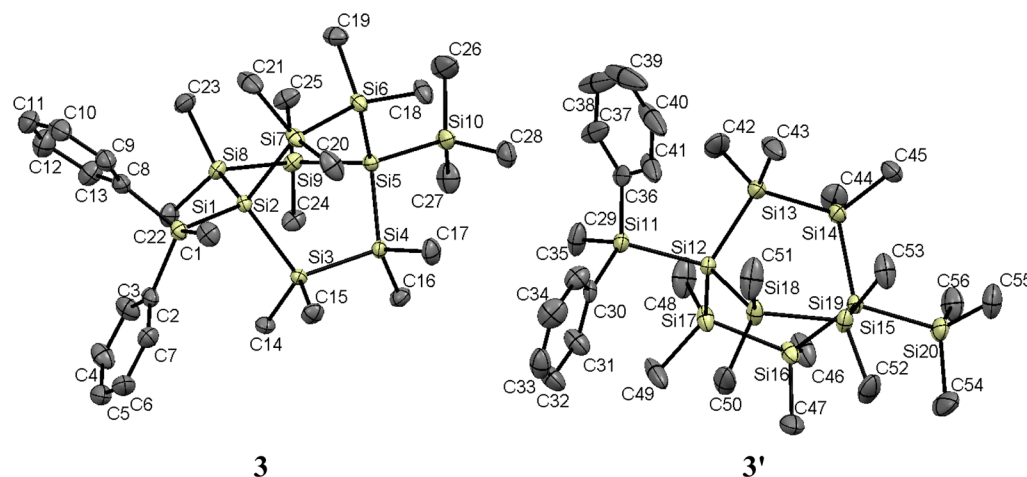


Figure 2. ORTEP diagram for compound 3. Thermal ellipsoids are depicted at the 50% probability level. Hydrogen atoms are omitted for clarity. The crystals contain two independent molecules (**3**, **3'**) in the asymmetric unit. Selected bond lengths [Å] and bond and torsional angles [deg] with estimated standard deviations: **3**: Si–Si (mean) 2.355, Si(1)–C(2) 1.889(3), Si(1)–C(8) 1.876(3), Si–C_{methyl} (mean) 1.887, Si–Si–Si (mean) 109.6, C(2)–Si(1)–Si(2) 112.30(9), C(8)–Si(1)–Si(2) 113.60(9), Si(2)–Si(3)–Si(4)–Si(5) –17.22(5), Si(2)–Si(7)–Si(6)–Si(5) –18.95(5), Si(2)–Si(8)–Si(9)–Si(5) –18.59(5), Si(2)–Si(1)–C(2)–C(3) –55.5(5), Si(2)–Si(1)–C(2)–C(7) 128.1(2), Si(2)–Si(1)–C(8)–C(9) –123.3(2), Si(2)–Si(1)–C(8)–C(13) 60.1(3). **3'**: Si–Si (mean) 2.354, Si(11)–C(30) 1.890(3), Si(11)–C(36) 1.881(3), Si–C_{methyl} (mean) 1.888, Si–Si–Si (mean) 109.8, C(30)–Si(11)–Si(12) 113.33(9), C(36)–Si(11)–Si(12) 109.3(1), Si(15)–Si(14)–Si(13)–Si(12) –14.11(5), Si(15)–Si(16)–Si(17)–Si(12) –18.43(6), Si(15)–Si(19)–Si(18)–Si(12) –17.16(6), Si(12)–Si(11)–C(30)–C(31) –68.7(2), Si(12)–Si(11)–C(30)–C(35) 114.6(2), Si(12)–Si(11)–C(36)–C(37) 117.7(3), Si(12)–Si(11)–C(36)–C(41) –61.1(3).

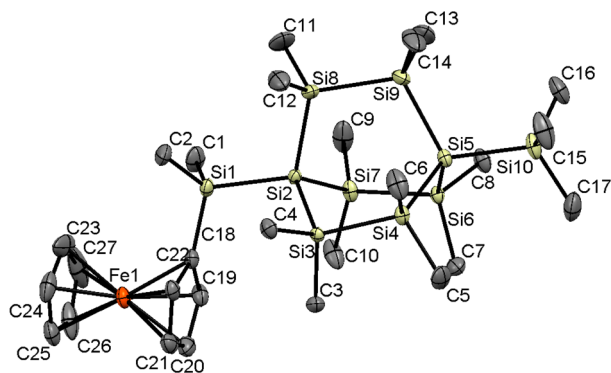


Figure 3. ORTEP diagram for compound 4. Thermal ellipsoids are depicted at the 50% probability level. Hydrogen atoms are omitted for clarity. Selected bond lengths [Å] and bond and torsional angles [deg] with estimated standard deviations: Si–Si (mean) 2.349, Si(1)–C(18) 1.862(2), Si–C_{methyl} (mean) 1.884, Si–Si–Si (mean) 109.6, Si(2)–Si(1)–C(18) 108.67(5), Si(2)–Si(3)–Si(4)–Si(5) –13.31(3), Si(2)–Si(7)–Si(6)–Si(5) –17.74(3), Si(2)–Si(8)–Si(9)–Si(5) –17.75(3), Si(2)–Si(1)–C(18)–C(19) –86.1(1), Si(2)–Si(1)–C(18)–C(22) 89.4(1).

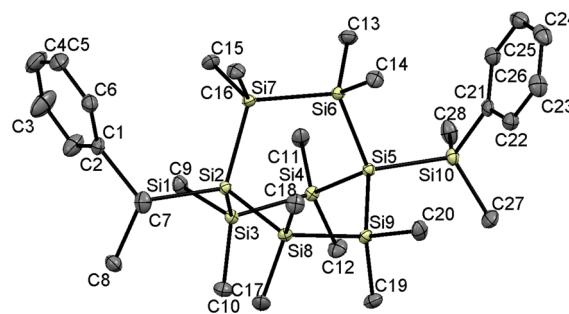


Figure 4. ORTEP diagram for compound 10. Thermal ellipsoids are depicted at the 50% probability level. Hydrogen atoms are omitted for clarity. Selected bond lengths [Å] and bond and torsional angles [deg] with estimated standard deviations: Si–Si (mean) 2.352, Si(1)–C(1) 1.886(2), Si(10)–C(21) 1.882(1), Si–C_{methyl} (mean) 1.886, Si–Si–Si (mean) 109.6, C(1)–Si(1)–Si(2) 109.86(5), C(21)–Si(10)–Si(5) 110.12(4), Si(2)–Si(3)–Si(4)–Si(5) 15.63(2), Si(5)–Si(6)–Si(7)–Si(2) 15.97(2), Si(2)–Si(8)–Si(9)–Si(5) 18.87(2), Si(2)–Si(1)–C(1)–C(2) 83.9(1), Si(2)–Si(1)–C(1)–C(6) –94.9(1), Si(5)–Si(10)–C(21)–C(22) 80.0(1), Si(5)–Si(10)–C(21)–C(26) –100.6(1).

1.92–1.94 Å are considerably elongated, the average Si–C(sp³) bond length was calculated from 19 169 individual XRD experimental values to be 1.860 Å.²¹ Significantly elongated Si–C bond distances in acyl silanes have been observed earlier,²² and it has been suggested that this lengthening of the silicon carbonyl group bond can be ascribed not only to contributions of canonical forms with single C–O bonds (Scheme 6, structure A), but also to a resonance structure without a formal bond between the metalloid atom and the carbonyl carbon (Scheme 6, structure B).²³ According to a more recent study, finally, the situation is best described by structure C with a dative bond between a negatively charged carbon and a positively charged silicon atom.²⁴

The silacarboxylic acid **9** afforded crystals of proper quality only from 2-propanol. The resulting crystals belong to the triclinic space group *P* $\bar{1}$ with two molecules in the unit cell, which are connected to dimers via hydrogen bridges by two molecules of 2-propanol (compare Figure 7).

There is only a minor impact of the substituents attached to the bridgehead silicons on the structure of the bicyclo[2.2.2]octasilane core. In line with structural data of bicyclo[2.2.2]octasilanes published earlier^{13,15b} the compounds investigated in this study exhibit a slightly twisted structure of the bicyclo[2.2.2]octasilane cage with nonparallel –Si₂Me₄– bridges in order to minimize steric repulsion. Endocyclic dihedral angles Si_{bridgehead}–Si–Si–Si_{bridgehead} range from 14.1° to 22.4°. Si–Si–Si bond angles close to the ideal tetrahedral angle between 105.8° and 111.5° and Si–Si bond lengths between 2.34 and 2.37 Å were

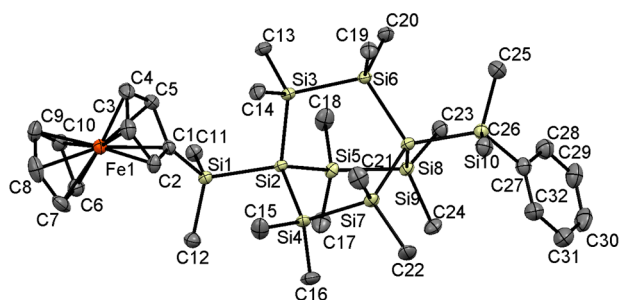


Figure 5. ORTEP diagram for compound **13**. Thermal ellipsoids are depicted at the 50% probability level. Hydrogen atoms are omitted for clarity. Selected bond lengths [Å] and bond and torsional angles [deg] with estimated standard deviations: Si–Si (mean) 2.353, Si(1)–C(1) 1.866(3), Si(10)–C(27) 1.885(3), Si–C_{methyl} (mean) 1.888, Si–Si–Si (mean) 109.7, C(1)–Si(1)–Si(2) 107.90(9), C(27)–Si(10)–Si(8) 110.21(9), Si(2)–Si(3)–Si(6)–Si(8) –15.80(5), Si(2)–Si(4)–Si(7)–Si(8) –17.74(5), Si(2)–Si(5)–Si(9)–Si(8) –14.84(5), Si(2)–Si(1)–C(1)–C(2) –84.4(2), Si(2)–Si(1)–C(1)–C(5) –93.3(2), Si(8)–Si(10)–C(27)–C(28) 90.2(2), Si(8)–Si(10)–C(27)–C(32) –87.6(3).

observed. The average Si–Si bond distance of 2.35 Å is typical for Si–Si single bonds in cyclopolysilanes²⁵ and agrees well with the Si–Si covalent bond length of 2.34 Å.

UV absorption spectra of **1**–**14** have been recorded in order to estimate the extent of interactions between the bridgehead substituents with the bicyclooctasilane Si–Si bond system. UV absorption data are summarized in Table 2.

Figure 8 compares the absorption spectrum of **1** with the spectra of the phenyl- and ferrocenyl-substituted compounds **2**, **3**, **4**, **10**, **11**, and **13**. The ferrocenylsilanes **4**, **11**, and **13** show characteristic weak absorption bands near 460 and 330 nm, which arise from local transitions within ferrocene.²⁶ All spectra exhibit additional bands in the near UV region. For **1** a typical shoulder appears at 240 nm, which previously has been assigned to $\sigma \rightarrow \pi^*$ type electron transitions involving the σ -SiSi skeleton.¹⁶ In the spectra of **2** and **4** this band is shifted considerably to the red by 20 and 30 nm, respectively. This behavior is usually observed when aromatic side groups are attached to permethylated oligosilane frameworks and is easily

rationalized if one assumes σ – π type hyperconjugative interactions between the aromatic π - and the SiSi σ -electrons.^{27,28} In the case of open-chained permethyloligosilanes the most striking red shift was found upon introduction of the first phenyl group, while a second phenyl substituent is much less effective. Thus, Me₃SiSiMe₂SiMe₃ exhibits a first absorption maximum at 216 nm,²⁹ which is shifted to 240 nm in PhMe₂SiSiMe₂SiMe₃³⁰ and to 243 nm in PhMe₂SiSiMe₂SiMe₂Ph.³¹ In line with this observation the absorption spectrum of **3** displays a 5 nm red shift of the first absorption maximum relative to **2**, while **10** and **11** show identical λ_{max} values as compared to **2** and **4**, respectively. Apparently the σ – π conjugated bond system within **2** and **4** is not extended further by the presence of the second aryl group, which makes any electronic coupling of the aromatic substituents via the bicyclooctasilane cage rather unlikely.

UV absorption spectra of the carbonyl derivatives **6**–**7** and **12** are depicted in Figure 9. The weak low-energy absorption bands in the spectra of compounds **6**, **7**, and **12** centered near 370 nm are typical for acylsilanes and can be assigned to symmetry-forbidden local $n \rightarrow \pi^*$ transitions within the C=O group. The position and intensity of these absorption maxima are nearly unaffected by the structure of the attached oligosilanyl moiety and compare closely with the values estimated for (Me₃Si)₃SiCOR or Me₃SiCOR.³² In general it is well established that β -silyl groups exert only little influence on the energies of $n \rightarrow \pi^*$ transitions in acyl silanes.³³ Otherwise the spectra are rather featureless. In the UV part strong maxima around 210 nm appear, which cannot be assigned without ambiguity either to carbonyl $\pi \rightarrow \pi^*$ or electron transitions within the polysilane skeleton. The silyl carboxylate **8** and the silyl carboxylic acid **9** exhibit a continuously rising absorption below 300 nm without any detectable maxima above 205 nm, which is characteristic for related systems.^{17c,34} Obviously in these species the carboxyl $n \rightarrow \pi^*$ absorption band that is found at 245 and 243 nm in the spectra of Me₃SiCOOMe and Me₃SiCOOH,³⁵ respectively, is completely masked by the polysilanyl absorption in the near-UV region.

As shown in Figure 10, finally, the absorption spectrum of **14** resembles the calculated sum spectrum of compounds **4** and **7**, which contain the separate chromophores. The spectrum of **14**,

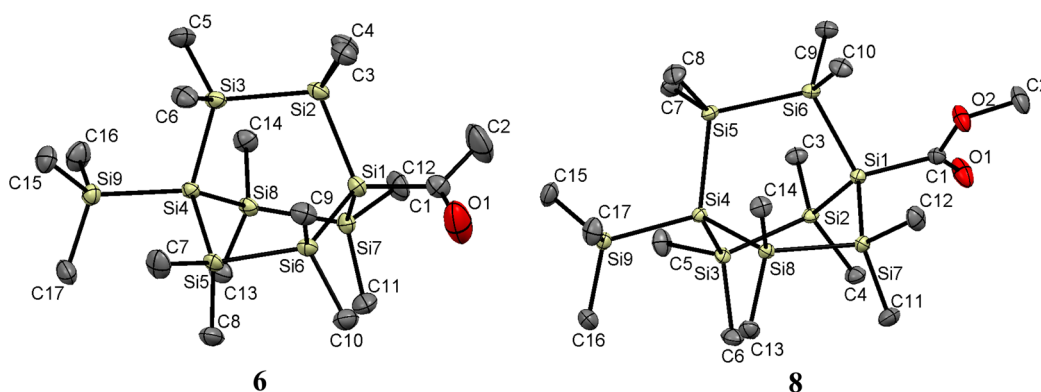


Figure 6. ORTEP diagram for compounds **6** and **8**. Thermal ellipsoids are depicted at the 50% probability level. Hydrogen atoms are omitted for clarity. Selected bond lengths [Å] and bond and torsional angles [deg] with estimated standard deviations: **6**: Si–Si (mean) 2.353, C(1)–O(1) 1.231(4), Si(1)–C(1) 1.917(4), Si–C_{methyl} (mean) 1.880, Si–Si–Si (mean) 109.1, O(1)–C(1)–C(2) 116.4(4), O(1)–C(1)–Si(1) 121.3(3), C(2)–C(1)–Si(1) 122.1(3), Si(1)–Si(2)–Si(3)–Si(4) –22.38(6), Si(4)–Si(5)–Si(6)–Si(1) –19.06(6), Si(4)–Si(8)–Si(7)–Si(1) –19.00(6). **8**: Si–Si (mean) 2.354, C(1)–O(1) 1.201(2), C(2)–O(2) 1.447(2), C(1)–O(2) 1.357(2), Si(1)–C(1) 1.935(2), Si–C_{methyl} (mean) 1.885, Si–Si–Si (mean) 109.0, O(1)–C(1)–O(2) 121.5(1), O(1)–C(1)–Si(1) 126.9(1), O(2)–C(1)–Si(1) 111.6(1), Si(1)–Si(2)–Si(3)–Si(4) 19.15(3), Si(4)–Si(5)–Si(6)–Si(1) 21.61(3), Si(4)–Si(8)–Si(7)–Si(1) 18.49(3), Si(1)–C(1)–O(2)–C(2) –178.7(1).

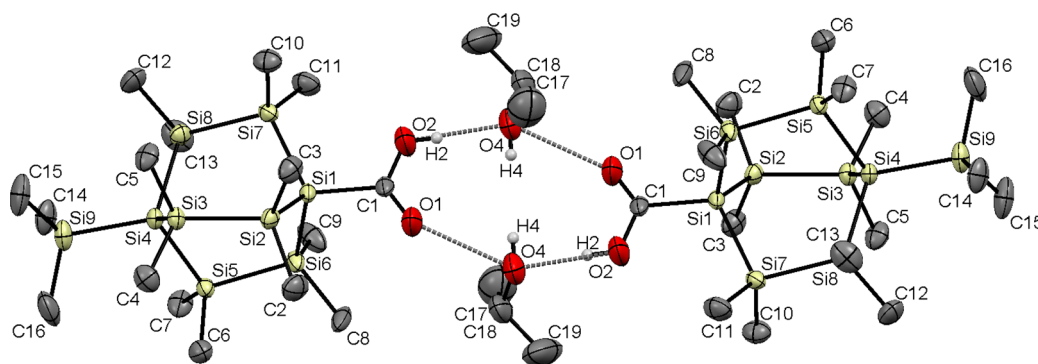


Figure 7. ORTEP diagram for compound **9**. Thermal ellipsoids are depicted at the 50% probability level. Hydrogen atoms are omitted for clarity. Selected bond lengths [Å] and bond and torsional angles [deg] with estimated standard deviations: Si–Si (mean) 2.347, C(1)–O(1) 1.194(6), C(1)–O(2) 1.311(6), Si(1)–C(1) 1.942(5), Si–C_{methyl} (mean) 1.880, O(2)–O(4) 2.661(8), O(1)–O(4) 2.807(8), Si–Si–Si (mean) 109.2, O(1)–C(1)–O(2) 122.2(4), O(1)–C(1)–Si(1) 123.2(4), O(2)–C(1)–Si(1) 114.5(3), Si(1)–Si(2)–Si(3)–Si(4) –16.60(8), Si(4)–Si(5)–Si(6)–Si(1) –17.02(9), Si(4)–Si(8)–Si(7)–Si(1) –20.57(9).

Scheme 6

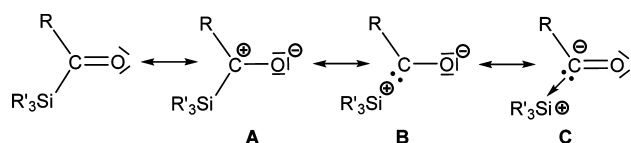


Table 2. Absorption Data for **1–14** (*n*-hexane solution, $c = 4 \times 10^{-5}$; 10^{-3} mol·L⁻¹)

	$\lambda_{\text{max, abs}}$ (nm) (ϵ (L·mol ⁻¹ ·cm ⁻¹))
1 ^a	240sh (16 000)
2	240sh (19 000), 260sh (8200)
3	265sh (10 500)
4	268 (14 900), 330sh (185), 458 (280)
6	213 (62 000), 265sh (6000), 359 (140), 372 (190), 387 (160)
7	212 (46 500), 370 (170)
8	only end absorption
9	only end absorption
10	258 (26 700)
11	268 (27 000), 325 (400), 458 (570)
12	232 (22 200), 371 (410)
13	260 (14 300), 332 (172), 457 (290)
14	270sh (15 000), 333 (260), 371 (240), 384 (237), 456 (315)

^aTaken from ref 15b.

therefore, seems to fulfill the classical expectation for nonconjugatively connected chromophores.

CONCLUSIONS

In summary, we have elaborated synthetic approaches toward bridgehead-functionalized permethylbicyclo[2,2,2]octasilanes. Starting from the corresponding 1-potassium and 1,4-dipotassium silanides previously unknown mono- and difunctional derivatives with COR, COOR, COOH, and SiMe_nR_m (R = Ph, Fc) attached to the bridgehead silicon atoms have been prepared successfully and fully characterized. In the crystalline state all compounds investigated in this study exhibit a slightly twisted structure of the bicyclooctasilane cage, which turned out to be remarkably insensitive toward the nature of the substituents attached to the bridgehead silicon atoms.

Except for the $n \rightarrow \pi^*$ absorption bands of the acyl silanes **6** and **7** centered near 370 nm, which exhibit nearly constant excitation energies as compared to Me₃SiCOR or

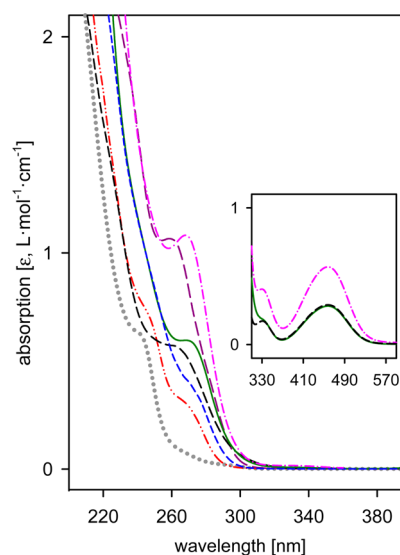


Figure 8. Absorption spectra of **1** and aryl-substituted bicyclo[2,2,2]-octasilanes (*n*-hexane solution; $c = 4 \times 10^{-5}$ M; inset $c = 10^{-3}$ M): (···, gray) **1**;^{15b} (---, red) **2**; (---, blue) **3**; (—, green) **4**; (— — —, purple) **10**; (---, magenta) **11**; (— — —, black) **13**.

(Me₃Si)₃SiCOR, the UV absorption spectra of the C=O derivatives **6–9** are rather featureless and, thus, do not allow drawing even qualitative conclusions concerning interactions between $\sigma(\text{SiSi})$ and C=O group orbitals. Due to $\sigma(\text{SiSi})/\pi(\text{aryl})$ conjugation, the absorption spectra of the phenyl and ferrocenyl derivatives show the expected bathochromic shift of the first UV absorption band relative to **1**. Attachment of another aryl substituent to the second terminal Me₃Si group, however, did not lead to further bathochromic shifts as observed in open-chained systems of comparable size. This allows us to conclude that there is no direct conjugational type interaction of the two aryl groups via the bicyclo[2,2,2]-octasilane skeleton, which can be rationalized using steric arguments. It has earlier been shown that cisoid conformations do not extend the conjugation within $\sigma(\text{SiSi})$ oligosilane skeletons.³⁶ Because the conjugation path going from one aryl group to the other via the octasilane cage contains one cisoid fragment, it is not surprising that conjugation between the two aryl groups leading to an extended conjugated system does not occur. This assumption is further supported by the observation

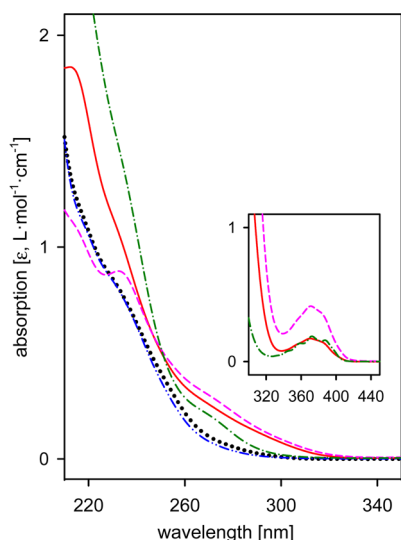


Figure 9. Absorption spectra of C=O-substituted bicyclo[2.2.2]octasilanes (*n*-hexane solution; $c = 4 \times 10^{-5}$ M; inset $c = 10^{-3}$ M). (---, green) 6; (—, red) 7; (-·-·, blue) 8; (···, black) 9; (- - - -, magenta) 12.

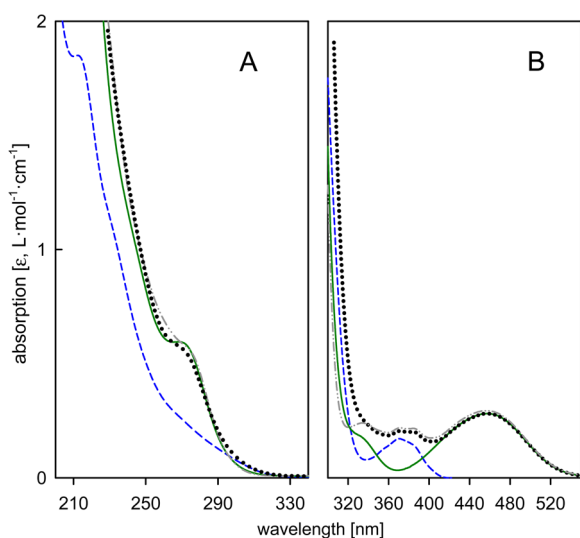


Figure 10. Comparison of absorption spectra of 4, 7, and 14 with the calculated sum of the spectra of 4 and 7. (A) UV part; *n*-hexane solution; $c = 4 \times 10^{-5}$ M; (B) visible part; $c = 10^{-3}$ M, (—, green) 4; (- - -, blue) 7; (-·-·) 14; (···) 4 + 7.

that the absorption spectrum of 14 resembles the calculated sum spectrum of compounds 4 and 7 and, thus, seems to fulfill the classical expectation for nonconjugatively connected chromophores.

EXPERIMENTAL SECTION

All experiments were performed under a nitrogen atmosphere using standard Schlenk techniques. Solvents were dried using a column solvent purification system.³⁷ KO t Bu (97%), MeCOCl (99%), t BuCOCl (99%), and ClCOOMe (98%) were used as purchased; Me₂SiCl₂ (98%) was distilled prior to use. Commercial CO₂ was dried by passing through P₂O₅. PhMe₂SiCl,³⁸ Ph₂MeSiCl,³⁹ FcMe₂SiCl,⁴⁰ 1-K, and 1-K₂^{12b} were synthesized as previously reported.¹H (299.95 MHz), ¹³C (75.43 MHz), and ²⁹Si (59.59 MHz) NMR spectra were recorded on a Varian INOVA 300 spectrometer in C₆D₆ solution and referenced versus TMS using the internal ²H-lock signal of the solvent. Mass spectra were run either on an HP 5971A/5890-II GC/MS

coupling (HP 1 capillary column, length 25 m, diameter 0.2 mm, 0.33 μ m poly(dimethylsiloxane)) or on a Kratos Profile mass spectrometer equipped with a solid probe inlet. Infrared spectra were obtained on a Bruker Alpha-P Diamond ATR spectrometer from the solid sample. UV–visible spectra were recorded in *n*-hexane solution, $c = 4 \times 10^{-5}$ and 10^{-3} mol·L⁻¹, respectively, on a Perkin-Elmer Lambda 35 spectrometer. Positions of absorption maxima and shoulders were obtained directly from the experimental spectra; absorptivity values ϵ were determined at the position of the maxima using Lambert–Beer's law. Melting points were determined using a Büchi 535 apparatus and are uncorrected. Elemental analyses were carried out on a Hanau Vario Elemental EL apparatus.

Synthesis of Dodecamethyl-4-(trimethylsilyl)-1-(dimethylphenylsilyl)bicyclo[2.2.2]octasilane (2). A solution of 1-K in 5 mL of DME was freshly prepared from 275 mg (0.5 mmol) of 1 and 62 mg (0.55 mmol) of KO t Bu. After removal of the volatile components in vacuo at room temperature the resulting residue was taken up in 10 mL of toluene, cooled to -70 °C, and slowly added to a solution of 102 mg (0.6 mmol) of PhMe₂SiCl in 20 mL of toluene. Subsequently the mixture was stirred for another 30 min and finally allowed to warm to room temperature. After aqueous workup with 100 mL of 10% sulfuric acid the organic layer was separated and dried over Na₂SO₄, and the solvent was stripped off with a rotary evaporator. Drying in vacuo (0.02 mbar) and crystallization from pentane by evaporation of the solvent at room temperature afforded 210 mg (69%) of white and crystalline 2.

Mp: 131–133 °C. Anal. Found: C, 44.12; H, 8.86. Calcd for C₂₃H₅₆Si₁₀: C, 45.02; H, 9.20. ²⁹Si NMR (CDCl₃, TMS, ppm): -6.05 (SiMe₃); -10.54 (SiMe₂Ph); -37.89 , -38.26 (SiMe₂); -129.04 (SiSiMe₂Ph); -131.00 (SiSiMe₃). ¹³C NMR (CDCl₃, TMS, ppm): 141.50, 133.98, 128.40, 127.67 (C₃H₆); 3.55 (Si(CH₃)₃); 1.70 (Si(CH₃)₂Ph); -1.17 , -1.31 (Si(CH₃)₂). ¹H NMR (CDCl₃, TMS, ppm, rel int): 7.32–7.55 (5H, m, (C₆H₅)); 0.55 (6H, s, Si(CH₃)₂Ph); 0.25 (18H, s, Si(CH₃)₂); 0.22 (9H, s, Si(CH₃)₃); 0.20 (18H, s, Si(CH₃)₂). HRMS: calcd for [C₂₃H₅₆Si₁₀]⁺ (M⁺) 612.2075; found 612.2104.

Synthesis of Dodecamethyl-4-(trimethylsilyl)-1-(methylphenylsilyl)bicyclo[2.2.2]octasilane (3). The procedure followed was that used for 2 with 715 mg (1.3 mmol) of 1, 160 mg (1.4 mmol) of KO t Bu, and 333 mg (1.4 mmol) of Ph₂MeSiCl. Crystallization of the crude product from diethyl ether/ethanol (1:1) by evaporation of the solvents at room temperature afforded 670 mg (76%) of white and crystalline 3.

Mp: 136–138 °C. ²⁹Si NMR (CDCl₃, TMS, ppm): -6.08 (SiMe₃); -11.81 (SiMePh₂); -37.76 , -38.18 (SiMe₂); -128.37 (SiSiMePh₂); -131.45 (SiSiMe₃). ¹³C NMR (CDCl₃, TMS, ppm): 138.91, 135.18, 128.71, 127.67 (C₃H₆); 3.48 (Si(CH₃)₃); 0.90 (SiCH₃Ph₂); -1.41 ($\times 2$, Si(CH₃)₂). ¹H NMR (CDCl₃, TMS, ppm, rel int): 7.62–7.33 (10H, m, (C₆H₅)); 0.82 (3H, s, SiCH₃Ph₂); 0.26 (18H, s, Si(CH₃)₂); 0.23 (9H, s, Si(CH₃)₃); 0.20 (18H, s, Si(CH₃)₂). HRMS: calcd for [C₂₈H₅₈Si₁₀]⁺ (M⁺) 674.2231; found 674.2265.

Synthesis of 1-(Ferrocenyldimethylsilyl)dodecamethyl-4-(trimethylsilyl)bicyclo[2.2.2]octasilane (4). To a solution of 1-K in 10 mL of DME (freshly prepared from 2.76 g (5 mmol) of 1 and 0.62 g (5.5 mmol) of KO t Bu) was slowly added a solution of 1.45 g (5.2 mmol) of FcSiMe₂Cl in 50 mL of DME at -50 °C. Subsequently the mixture was stirred for another 30 min and finally allowed to warm to room temperature. After aqueous workup with 10% sulfuric acid the organic layer was separated and dried over Na₂SO₄, and the volatile components were stripped off with a rotary evaporator. Drying in vacuo (0.02 mbar) and crystallization from diethyl ether/acetone (1:1) by evaporation of the solvents at room temperature afforded 2.83 g (78%) of orange and crystalline 4.

Mp: 186–187 °C. Anal. Found: C, 44.35; H, 8.28. Calcd for C₂₇H₆₁FeSi₁₀: C, 44.95; H, 8.38. ²⁹Si NMR (CDCl₃, TMS, ppm): -6.11 (SiMe₃); -11.45 (SiMe₂Fc); -38.12 , -38.31 (SiMe₂); -128.90 (SiSiMe₂Fc); -130.67 (SiSiMe₃). ¹³C NMR (CDCl₃, TMS, ppm): 74.92, 73.37, 70.75 (C₃H₄–SiMe₂); 68.17 (C₅H₅); 3.51 (Si(CH₃)₃); 1.95 (Si(CH₃)₂Fc); -1.27 , -1.34 (Si(CH₃)₂). ¹H NMR (CDCl₃, TMS, ppm, rel int): 4.35, 4.10 (4H, b, Si(C₃H₄)); 4.17 (5H, s, C₃H₅);

0.51 (6H, s, Si(CH₃)₂(C₅H₄)); 0.23 (18H, s, Si(CH₃)₂); 0.21 (9H, s, Si(CH₃)₃); 0.17 (18H, s, Si(CH₃)₂). HRMS: calcd for [C₂₇H₆₀Si₁₀Fe]⁺⁺ (M⁺) 720.1739; found 720.1785.

Synthesis of 1-(Chlorodimethylsilyl)dodecamethyl-4-(trimethylsilyl)bicyclo[2.2.2]octasilane (5). A solution of **1-K** in 5 mL of DME was freshly prepared from 2.21 g (4 mmol) of **1** and 0.42 g (4.2 mmol) of KOtBu. After removal of the volatile components in vacuo at room temperature the resulting residue was taken up in 5 mL of toluene, cooled to -70 °C, and slowly added to a solution of 2.06 g (16 mmol) of Me₂SiCl₂ in 20 mL of toluene. Subsequently the mixture was stirred for another 30 min and finally allowed to warm to room temperature. After removal of the volatile components in vacuo (0.02 mbar) the solid residue was taken up with 20 mL of heptane and filtered over Celite. Removal of the solvent from the filtrate and drying in vacuo at room temperature afforded 2.13 g (93%) of pure **5** as colorless crystals.

Mp: 155–157 °C (dec). Anal. Found: C, 35.72; H, 8.78. Calcd for C₁₇H₅₁ClSi₁₀: C, 35.70; H, 8.99. ²⁹Si NMR (CDCl₃, TMS, ppm): 33.27 (SiMe₂Cl); -6.13 (SiMe₃); -38.21, -38.42 (SiMe₂); -125.01 (SiSiMe₂Cl); -130.48 (SiSiMe₃). ¹³C NMR (CDCl₃, TMS, ppm): 8.24 (Si(CH₃)₂Cl); 3.37 (Si(CH₃)₃); -1.34, -1.66 (Si(CH₃)₂). ¹H NMR (CDCl₃, TMS, ppm, rel int): 0.58 (6H, s, Si(CH₃)₂Cl); 0.37, (18H, s, Si(CH₃)₂); 0.31 (18H, s, Si(CH₃)₂); 0.26 (9H, s, Si(CH₃)₃). MS: calcd for [C₁₇H₅₁ClSi₁₀]⁺⁺ (M⁺) 570.2; found 570.3.

Synthesis of 1-Acyl-4-(trimethylsilyl)-dodecamethylbicyclo[2.2.2]octasilane (6). A solution of **1-K** in 10 mL of DME (freshly prepared from 2.21 g (4 mmol) of **1** and 0.49 g (4.4 mmol) of KOtBu) was slowly added to a solution of 0.33 g (4.2 mmol) of MeCOCl in 40 mL of diethyl ether at -80 °C. Subsequently the mixture was stirred for an additional hour at -80 °C and finally allowed to warm to room temperature. After aqueous workup with 100 mL of 2% sulfuric acid the organic layer was separated and dried over Na₂SO₄, and the solvent was stripped off with a rotary evaporator. The resulting oily residue was chromatographed (toluene/heptane, 10:1, silica gel) to give **6** (0.88 g, 42%) as a white solid. Crystals suitable for X-ray structure analysis could be grown from acetone solution by evaporation of the solvent at room temperature.

Mp: 60 °C (dec). ²⁹Si NMR (CDCl₃, TMS, ppm): -5.65 (SiMe₃); -38.05, -39.76 (SiMe₂); -72.68 (SiCOMe), -129.78 ppm (SiSiMe₃). ¹³C NMR (CDCl₃, TMS, ppm): 244.06 (COCH₃); 42.69 (COCH₃); 3.48 (Si(CH₃)₃); -1.38, -2.78 (Si(CH₃)₂). ¹H NMR (CDCl₃, TMS, ppm, rel int): 2.30 (3H, s, COCH₃); 0.34 (18H, s, Si(CH₃)₂); 0.30 (18H, s, Si(CH₃)₂); 0.24 (9H, s, Si(CH₃)₃). IR (neat): ν(C=O) = 1632 (m) cm⁻¹. HRMS: calcd for [C₁₇H₄₈OSi₉]⁺⁺ (M⁺) 520.1628; found 520.1653.

Synthesis of 1-Trimethylacyl-4-(trimethylsilyl)-dodecamethylbicyclo[2.2.2]octasilane (7). The procedure followed was that used for **6** with 825 mg (1.5 mmol) of **1**, 179 mg (1.6 mmol) of KOtBu, and 192 mg (1.6 mmol) of tBuCOCl. Yield: 740 mg (88%) of a colorless solid, which gave 520 mg (61%) of pure and crystalline **7** after recrystallization from acetone by evaporation of the solvent at room temperature.

Mp: 202–204 °C (dec). ²⁹Si NMR (CDCl₃, TMS, ppm): -5.83 (SiMe₃); -37.76, -38.09 (SiMe₂); -75.68 (SiCOtBu), -130.82 ppm (SiSiMe₃). ¹³C NMR (CDCl₃, TMS, ppm): 247.64 (COtBu); 48.41 (COCMe₃); 24.67 (C(CH₃)₃); 3.46 (Si(CH₃)₃); -1.19, -1.90 (Si(CH₃)₂). ¹H NMR (CDCl₃, TMS, ppm, rel int): 1.04 (9H, s, C(CH₃)₃); 0.32 (18H, s, Si(CH₃)₂); 0.30 (18H, s, Si(CH₃)₂); 0.24 (9H, s, Si(CH₃)₃). IR (neat): ν(C=O) = 1622 (m) cm⁻¹. HRMS: calcd for [C₂₀H₅₄OSi₉]⁺⁺ (M⁺) 652.2098; found 562.2119.

Synthesis of 1-Methylcarboxy-4-(trimethylsilyl)-dodecamethylbicyclo[2.2.2]octasilane (8). The procedure followed was that used for **6** with 550 mg (1.0 mmol) of **1**, 123 mg (1.1 mmol) of KOtBu, and 470 mg (5 mmol) of ClCOOMe. Recrystallization of the resulting resinous residue from ethanol by evaporation of the solvent at room temperature afforded 490 mg (89%) of white and crystalline **8**.

Mp: 60 °C (dec). Anal. Found: C, 37.26; H, 8.40. Calcd for C₁₇H₄₈O₂Si₉: C, 38.00; H, 9.00. ²⁹Si NMR (CDCl₃, TMS, ppm): -5.52 (SiMe₃); -38.09, -39.19 (SiMe₂); -76.68 (SiCOOMe),

-129.63 ppm (SiSiMe₃). ¹³C NMR (CDCl₃, TMS, ppm): 187.77 (COOCH₃); 49.13 (COOCH₃); 3.57 (Si(CH₃)₃); -1.32, -3.05 (Si(CH₃)₂). ¹H NMR (CDCl₃, TMS, ppm, rel int): 3.63 (3H, s, COOCH₃); 0.33 (18H, s, Si(CH₃)₂); 0.31 (18H, s, Si(CH₃)₂); 0.25 (9H, s, Si(CH₃)₃). IR (neat): ν(C=O) = 1662 (m) cm⁻¹. HRMS: calcd for [C₁₇H₄₈O₂Si₉]⁺⁺ (M⁺) 536.1578; found 536.1600.

Synthesis of Dodecamethyl-4-trimethylsilylbicyclo[2.2.2]octasilanyl-1-carboxylic Acid (9). A solution of **1-K** in 10 mL of DME (freshly prepared from 3.31 g (6 mmol) of **1** and 740 mg (6.6 mmol) of KOtBu) was slowly added at -70 °C to a saturated solution of CO₂ in diethyl ether, which has been obtained by slowly bubbling thoroughly dried CO₂ through 150 mL of diethyl ether at -70 °C for 20 min. Subsequently the mixture was stirred for another 30 min at -70 °C and finally allowed to warm to room temperature. After aqueous workup with 100 mL of 2% sulfuric acid the organic layer was separated and dried over Na₂SO₄, and the volatile components were removed with a rotary evaporator. Subsequent drying at 0.02 mbar afforded 301 mg (96%) of pure **9** as a white, moderately air-stable powder. Crystals suitable for X-ray structure analysis were obtained after recrystallization from 2-propanol by evaporation of the solvent at room temperature.

Mp: 163–165 °C (dec). Anal. Found: C, 36.08; H, 8.28. Calcd for C₁₆H₄₆O₃Si₉: C, 36.72; H, 8.86. ²⁹Si NMR (CDCl₃, TMS, ppm): -5.49 (SiMe₃); -38.12, -39.22 (SiMe₂); -76.72 (SiCOOH), -129.61 ppm (SiSiMe₃). ¹³C NMR (CDCl₃, TMS, ppm): 193.10 (COOH); 3.58 (Si(CH₃)₃); -1.31, -3.07 (Si(CH₃)₂). ¹H NMR (CDCl₃, TMS, ppm, rel int): 0.36 (18 H, s, Si(CH₃)₂); 0.32 (18H, s, Si(CH₃)₂); 0.25 (9H, s, Si(CH₃)₃). IR (neat): ν(O-H) = 3200–2500 (m) cm⁻¹; ν(C=O) = 1631 (m) cm⁻¹. HRMS: calcd for [C₁₆H₄₆O₃Si₉]⁺⁺ ([M - H]⁺) 521.1343; found 521.1346.

Synthesis of 1,4-Bis(dimethylphenylsilyl)-dodecamethylbicyclo[2.2.2]octasilane (10). A solution of **1-K**₂ in 10 mL of toluene (freshly prepared from 276 mg (0.5 mmol) of **1**, 123 mg (1.1 mmol) of KOtBu, and 291 mg (1.1 mmol) of 18-crown-6) was slowly added to a solution of 170 mg (1.0 mmol) of PhMe₂SiCl in 40 mL of toluene at -70 °C. Subsequently the mixture was stirred for another 30 min at -70 °C and finally allowed to warm to room temperature. After aqueous workup with 100 mL of 3% sulfuric acid the organic layer was separated and dried over Na₂SO₄, and the solvent was stripped off with a rotary evaporator. Drying in vacuo (0.02 mbar) and crystallization from pentane by evaporation of the solvent at room temperature afforded 220 mg (65%) of colorless and crystalline **10**.

Mp: 181–182 °C. Anal. Found: C, 49.72; H, 8.17. Calcd for C₂₈H₅₈Si₁₀: C, 49.78; H, 8.65. ²⁹Si NMR (CDCl₃, TMS, ppm): -10.60 (SiMe₂Ph); -37.90 (SiMe₂); -129.73 (SiSiMe₂Ph). ¹³C NMR (CDCl₃, TMS, ppm): 141.42, 133.94, 128.39, 127.66 (C₆H₅); 1.64 (Si(CH₃)₂Ph); -1.36 (Si(CH₃)₂). ¹H NMR (CDCl₃, TMS, ppm, rel int): 7.53–7.31 (10H, m, (C₆H₅)); 0.54 (12H, s, Si(CH₃)₂Ph); 0.17 (36H, s, Si(CH₃)₂). HRMS: calcd for [C₂₈H₅₈Si₁₀]⁺⁺ (M⁺): 674.2231; found: 647.2247.

Synthesis of 1,4-Bis(ferrocenyldimethylsilyl)-dodecamethylbicyclo[2.2.2]octasilane (11). The procedure followed was that used for **10** with 1.00 g (1.8 mmol) of **1**, 0.43 g (3.8 mmol) of KOtBu, 1.15 g (3.8 mmol) of 18-crown-6, and 1.15 g (4.1 mmol) of FcMe₂SiCl. Crystallization of the crude product from diethyl ether by evaporation of the solvent at room temperature afforded 320 mg (20%) of orange and crystalline **11**.

Mp: 290 °C (dec). Anal. Found: C, 47.92; H, 7.02. Calcd for C₃₆H₆₈Fe₂Si₁₀: C, 48.39; H, 7.67. ²⁹Si NMR (CDCl₃, TMS, ppm): -11.40 (SiMe₂Fc); -38.14 (SiMe₂); -129.12 (SiSiMe₂Fc). ¹³C NMR (CDCl₃, TMS, ppm): 74.61, 73.16, 70.51 (C₅H₄-SiMe₂), 67.92 (C₅H₅); 1.92 (Si(CH₃)₂Fc); -1.39 (Si(CH₃)₂). ¹H NMR (CDCl₃, TMS, ppm, rel int): 4.31, 4.05 (8H, b, C₅H₄-SiMe₂); 4.14 (10H, b, C₅H₅); 0.51 (12H, s, Si(CH₃)₂Fc); 0.13 (36H, s, Si(CH₃)₂). HRMS: calcd for [C₃₆H₆₆Si₁₀Fe₂]⁺⁺ (M⁺) 890.1561; found 890.1549.

Synthesis of 1,4-Bis(trimethylacyl)-dodecamethylbicyclo[2.2.2]octasilane (12). Method a: The procedure followed was that used for **10** with 276 mg (0.5 mmol) of **1**, 123 mg (1.1 mmol) of KOtBu, 291 mg (1.1 mmol) of 18-crown-

6, and 132 mg (1.1 mmol) of ClCOtBu . Crystallization of the crude product from acetone at $-30\text{ }^\circ\text{C}$ afforded 140 mg (48%) of white and crystalline **12**.

Method b: 282 mg (0.5 mmol) of **7** was stirred with 62 mg (1.1 mmol) of KOtBu in 10 mL of DME for 40 min at room temperature. At this time ^{29}Si NMR analysis revealed quantitative formation of the silanide **7-K**. The resulting red solution was slowly added to a solution of 66 mg (0.55 mmol) of ClCOtBu in 10 mL of diethyl ether at $-70\text{ }^\circ\text{C}$. Subsequently the mixture was stirred for another 30 min at $-70\text{ }^\circ\text{C}$ and finally allowed to warm to room temperature. After stirring for an additional 2 h aqueous workup was accomplished by addition of 100 mL of 3% sulfuric acid, separation of the organic layer, drying over Na_2SO_4 , and removal of the solvent with a rotary evaporator. Crystallization of the oily residue from acetone/pentane (1:1) by evaporation of the solvents at room temperature afforded 90 mg (32%) of **12**.

7-K: ^{29}Si NMR ($\text{DME}/\text{D}_2\text{O}$, TMS, ppm): -33.05 ; -40.06 (SiMe_2); -73.86 (SiCOtBu); -180.69 (SiK).

12: Mp: $218\text{--}219\text{ }^\circ\text{C}$ (dec). ^{29}Si NMR (CDCl_3 , TMS, ppm): -37.59 (SiMe_2); -76.88 (SiCOtBu). ^{13}C NMR (CDCl_3 , TMS, ppm): 247.09 ($\text{COC}(\text{CH}_3)_3$), 48.45 ($\text{COC}(\text{CH}_3)_3$), 24.63 ($\text{COC}(\text{CH}_3)_3$), -1.88 ($\text{Si}(\text{CH}_3)_2$). ^1H NMR (CDCl_3 , TMS, ppm, rel int): 1.04 (18H, s, $\text{C}(\text{CH}_3)_3$), 0.34 (36H, s, $\text{Si}(\text{CH}_3)_3$). IR (neat): $\nu(\text{C}=\text{O}) = 1621\text{ cm}^{-1}$ (m). HRMS: calcd for $[\text{C}_{22}\text{H}_{34}\text{O}_2\text{Si}_8]^+$ (M^+) 574.2278 ; found 574.2303 .

Synthesis of 1-(Ferrocenyldimethylsilyl)-4-(dimethylphenylsilyl)dodecamethylbicyclo[2.2.2]octasilane (13). A 360 mg (0.5 mmol) sample of **4** was stirred with 62 mg (0.55 mmol) of KOtBu in 5 mL of DME for 40 min at room temperature. At this time ^{29}Si NMR analysis of the resulting red solution revealed quantitative formation of the silanide **4-K**. The resulting red solution was slowly added to a solution of 940 mg (0.55 mmol) of PhMe_2SiCl in 10 mL of diethyl ether at $-70\text{ }^\circ\text{C}$. Subsequently the mixture was stirred for another 30 min at $-70\text{ }^\circ\text{C}$ and finally allowed to warm to room temperature. After stirring for an additional 2 h aqueous workup was accomplished by addition of 100 mL of 3% sulfuric acid, separation of the organic layer, drying over Na_2SO_4 , and removal of the solvent with a rotary evaporator. Crystallization of the oily residue from acetone at $-30\text{ }^\circ\text{C}$ afforded 310 mg (80%) of red and solid **13**. The product can be purified further by column chromatography (hexane, silica gel). Yield: 230 mg (59%).

4-K: ^{29}Si NMR ($\text{DME}/\text{D}_2\text{O}$, TMS, ppm): 6.58 ($\text{Me}_2\text{Si-OtBu}$); -11.71 (SiMe_2Fc); -34.32 , -39.67 (SiMe_2); -127.89 (SiSiMe_2Fc); -177.62 (SiK).

13: Mp: $153\text{--}156\text{ }^\circ\text{C}$. Anal. Found: C, 48.71; H, 7.55. Calcd for $\text{C}_{32}\text{H}_{62}\text{FeSi}_{10}$: C, 49.05; H, 7.98. ^{29}Si NMR (CDCl_3 , TMS, ppm): -10.59 (SiMe_2Ph); -11.60 (SiMe_2Fc); -37.89 , -38.09 (SiMe_2); -129.28 , -129.55 (SiSiMe_2Ph , SiSiMe_2Fc). ^{13}C NMR (CDCl_3 , TMS, ppm): 141.52 , 133.96 , 128.38 , 127.66 (C_6H_5); 75.23 , 73.85 , 71.02 ($\text{C}_5\text{H}_4\text{-SiMe}_2$); 68.42 (C_5H_5); 1.95 , 1.65 ($\text{Si}(\text{CH}_3)_2\text{Ph}$, $\text{Si}(\text{CH}_3)_2\text{Fc}$); -1.34 , -1.36 ($\text{Si}(\text{CH}_3)_2$). ^1H NMR (CDCl_3 , TMS, ppm, rel int): $7.54\text{--}7.32$ (5H, m, (C_6H_5)); 4.18 (5H, b, (C_5H_5)); 4.35 , 4.10 (4H, b, (C_5H_4)- SiMe_2); 0.55 (12H, b, $\text{Si}(\text{CH}_3)_2\text{Ph}$, $\text{Si}(\text{CH}_3)_2\text{Fc}$); 0.18 , (36H, b, $\text{Si}(\text{CH}_3)_2$). HRMS: calcd for $[\text{C}_{32}\text{H}_{62}\text{Si}_{10}\text{Fe}]^+$ (M^+) 782.1896 ; found 782.1866 .

Synthesis of 1-(Ferrocenyldimethylsilyl)-4-(trimethylacetyl)dodecamethylbicyclo[2.2.2]octasilane (14). The procedure followed was that used for **13** with 360 mg (0.5 mmol) of **4**, 62 mg (0.55 mmol) of KOtBu , and 66 mg (0.55 mmol) of ClCOtBu . After removal of the solvents, washing of the crude product with acetone, and drying in vacuo (0.02 mbar) 280 mg (78%) of pure **14** was obtained as an orange powder.

Mp: $219\text{--}221\text{ }^\circ\text{C}$ (dec). Anal. Found: C, 46.82; H, 7.93. Calcd for $\text{C}_{29}\text{H}_{60}\text{FeOSi}_9$: C, 47.49; H, 8.25. ^{29}Si NMR (CDCl_3 , TMS, ppm): -11.33 (SiMe_2Fc); -37.54 , -38.10 (SiMe_2); -76.00 (SiCOtBu); -129.59 (SiSiMe_2Fc). ^{13}C NMR (CDCl_3 , TMS, ppm): 247.74 (CO); 74.23 , 73.15 , 70.65 ($\text{C}_5\text{H}_4\text{-SiMe}_2$); 68.00 (C_5H_5); 48.39 ($\text{C}(\text{CH}_3)_3$); 24.66 ($\text{C}(\text{CH}_3)_3$); 1.90 ($\text{Si}(\text{CH}_3)_2\text{Fc}$); -1.33 , -1.93 ($\text{Si}(\text{CH}_3)_2$). ^1H NMR (CDCl_3 , TMS, ppm, rel int): 4.18 (5H, b, (C_5H_5)); 4.36 , 4.10 (4H, b, (C_5H_4)- SiMe_2); 1.02 (9H, s, $\text{C}(\text{CH}_3)_3$), 0.52 (6H, s,

$\text{Si}(\text{CH}_3)_2\text{Fc}$); 0.28 , 0.20 (36H, s, $\text{Si}(\text{CH}_3)_2$). IR (neat): $\nu(\text{C}=\text{O}) = 1621\text{ cm}^{-1}$ (m). HRMS: calcd for $[\text{C}_{29}\text{H}_{60}\text{FeOSi}_9]^+$ (M^+) 732.1919 ; found 732.1945 .

X-ray Crystallography. For X-ray structure analysis suitable crystals were mounted onto the tip of glass fibers using mineral oil. Data collection was performed on a Bruker Kappa Apex II CCD diffractometer at 100 K for compounds **2**, **3**, **4**, **6**, **8**, **10**, and **13** and 200 K for compound **9** using graphite-monochromated $\text{Mo K}\alpha$ ($\lambda = 0.71073\text{ \AA}$) radiation. Details of the crystal data and structure refinement are provided as Supporting Information. The SHELX version 6.1 program package was used for the structure solution and refinement.⁴¹ Absorption corrections were applied using the SADABS program.⁴² All non-hydrogen atoms were refined with anisotropic displacement parameters. Hydrogen atoms were included in the refinement at calculated positions using a riding model as implemented in the SHELXTL program. Crystallographic data (excluding structure factors) have been deposited with the Cambridge Crystallographic Data Centre as supplementary publications CCDC-923021 (**2**), CCDC-923023 (**3**), CCDC-923022 (**4**), CCDC-923018 (**6**), CCDC-923020 (**8**), CCDC-923019 (**9**), CCDC-923017 (**10**), and CCDC-923016 (**13**). Copies of the data can be obtained free of charge on application to The Director, CCDC, 12 Union Road, Cambridge CB2 1EZ, UK (fax (internat.) +44-1223/336-033; e-mail deposit@ccdc.cam.ac.uk).

■ ASSOCIATED CONTENT

📄 Supporting Information

^1H and ^{29}Si NMR spectra of **3**, **6**, **7**, and **12**. Tables and CIF files giving crystal, collection, and refinement data for the structures of compounds **2**, **3**, **4**, **6**, **8**, **10**, and **13**. This material is available free of charge via the Internet at <http://pubs.acs.org>.

■ AUTHOR INFORMATION

✉ Corresponding Author

*Tel: +43/316/873-32111. Fax: +43/316-32102. E-mail: harald.stueger@tugraz.at.

Notes

The authors declare no competing financial interest.

■ ACKNOWLEDGMENTS

We thank the FWF (Wien, Austria) for financial support (project number P21271-N19).

■ REFERENCES

- (1) For leading reviews on oligo- and polysilanes see: (a) Krempner, C. *Polymers* **2012**, *4*, 408. (b) Feigl, A.; Bockholt, A.; Weis, J.; Rieger, B. *Adv. Polym. Sci.* **2011**, *235*, 1. (c) Semenov, V. V. *Russ. Chem. Rev.* **2011**, *80*, 313. (d) Nanjo, M.; Sekiguchi, A. In *Silicon-Containing Dendritic Polymers*; Dvornic, P., Owen, M. J., Eds.; Springer Science + Business Media B. V., 2009; Vol. 2, pp 75–96. (e) Beckmann, J. In *Comprehensive Organometallic Chemistry III*, Vol. 3; Crabtree, R. H.; Mingos, D. M. P.; Housecroft, C. E., Eds.; Elsevier: Amsterdam, 2007; p 409. (f) Marschner, C. *Organometallics* **2006**, *25*, 2110. (g) Fogarty, H. A.; Casher, D. L.; Imhof, R.; Schepers, T.; Rooklin, D. W.; Michl, J. *Pure Appl. Chem.* **2003**, *75*, 999. (h) Kira, M.; Miyazawa, T. In *The Chemistry of Organic Silicon Compounds*, Vol. 2; Rappoport, Z.; Apeloig, Y., Eds.; Wiley: Chichester, 1998; p 1311. (i) Hengge, E.; Stueger, H. In *The Chemistry of Organic Silicon Compounds*, Vol. 2; Rappoport, Z.; Apeloig, Y., Eds.; Wiley: Chichester, 1998; p 2177. (j) West, R. In *Comprehensive Organometallic Chemistry II*, Vol. 2; Wilkinson, G.; Stone, F. G. A.; Abel, E. W., Eds.; Pergamon Press, 1995; p 77. (k) Miller, R. D.; Michl, J. *Chem. Rev.* **1989**, *89*, 1359. (l) West, R. In *The Chemistry of Organic Silicon Compounds*; Patai, S.; Rappoport, Z., Eds.; Wiley: Chichester, 1989; p 1207. (m) West, R. In *Comprehensive Organometallic Chemistry*; Abel, E., Ed.; Pergamon Press, 1982; p 365. (2) West, R. *Pure Appl. Chem.* **1982**, *54*, 1041.

- (3) (a) Zirngast, M.; Baumgartner, J.; Marschner, C. *Organometallics* **2008**, *27*, 6472. (b) Stueger, H.; Hengge, E. *Monatsh. Chem.* **1988**, *119*, 873. (c) Carberry, E.; West, R.; Glass, G. E. *J. Am. Chem. Soc.* **1969**, *91*, 5446.
- (4) (a) Stueger, H.; Fuerpass, G.; Renger, K. *Organometallics* **2005**, *24*, 6374. (b) Kyushin, S.; Sakurai, H.; Yamaguchi, H.; Goto, M.; Matsumoto, H. *Chem. Lett.* **1995**, 815.
- (5) Grogger, C.; Rautz, H.; Stueger, H. *Monatsh. Chem.* **2001**, *132*, 453.
- (6) Ishikawa, M.; Kumada, M. *J. Chem. Soc. D: Chem. Commun.* **1970**, 612.
- (7) Rautz, H.; Stueger, H.; Kickelbick, G.; Pietzsch, C. *J. Organomet. Chem.* **2001**, *667*, 167.
- (8) Ref 1c contains an up-to-date compilation of known methods for polysilane synthesis including extensive bibliography.
- (9) Ref 1i, p 2205ff.
- (10) West, R.; Indriksons, A. *J. Am. Chem. Soc.* **1972**, *94*, 6110.
- (11) Setaka, W.; Hamada, N.; Kira, M. *Chem. Lett.* **2004**, *33*, 626.
- (12) (a) Marschner, C.; Baumgartner, J.; Wallner, A. *Dalton Trans.* **2006**, 5667. (b) Fischer, R.; Konopa, T.; Ully, S.; Baumgartner, J.; Marschner, C. *J. Organomet. Chem.* **2003**, *685*, 79.
- (13) Setaka, W.; Hamada, N.; Kabuto, C.; Kira, M. *Chem. Commun.* **2005**, 4566.
- (14) Kira, M. Personal unpublished communication.
- (15) (a) Wallner, A.; Hlina, J.; Konopa, T.; Wagner, H.; Baumgartner, J.; Marschner, C. *Organometallics* **2010**, *29*, 2660. (b) Wallner, A.; Hölbling, M.; Baumgartner, J.; Marschner, C. *Silicon Chem.* **2005**, *3*, 175.
- (16) Wallner, A.; Emanuelsson, R.; Baumgartner, J.; Marschner, C.; Ottosson, H. *Organometallics* **2013**, *32*, 396.
- (17) (a) Marschner, C. *Eur. J. Inorg. Chem.* **1998**, 221. (b) Mallela, S. P.; Ghuman, M. A.; Geanangel, R. A. *Inorg. Chim. Acta* **1992**, *202*, 211. (c) Brook, A. G.; Yau, L. *J. Organomet. Chem.* **1984**, *271*, 9. (d) Brook, A. G.; Harris, J. W.; Lennon, J.; El Sheikh, M. *J. Am. Chem. Soc.* **1979**, *101*, 83.
- (18) Kira, M.; Miyazawa, T.; Mikami, N.; Sakurai, H. *Organometallics* **1991**, *10*, 3793.
- (19) Tsuji, H.; Shibano, Y.; Takahashi, T.; Kumada, M.; Tamao, K. *Bull. Chem. Soc. Jpn.* **2005**, *78*, 1334.
- (20) (a) Berry, R. J.; Waltman, R. J.; Pacansky, J.; Hagler, A. T. *J. Phys. Chem.* **1995**, *99*, 10511. (b) Kanters, J. A.; Kroon, J.; Peerdeman, A. F.; Schoone, J. C. *Tetrahedron* **1967**, *23*, 4027.
- (21) Kaftory, M.; Kapon, M.; Botoshansky, M. In *The Chemistry of Organic Silicon Compounds*, Vol. 2; Rappoport, Z.; Apeloig, Y., Eds.; Wiley: Chichester, 1998; p 192.
- (22) Bulman-Page, P. C.; McKenzie, M. J.; Klair, S. S.; Rosenthal, S. In *The Chemistry of Organic Silicon Compounds*, Vol. 2; Rappoport, Z.; Apeloig, Y., Eds.; Wiley: Chichester, 1998; p 1605.
- (23) (a) Chieh, P. C.; Trotter, J. *J. Chem. Soc.* **1969**, 1778. (b) Harrison, R. W.; Trotter, J. *J. Chem. Soc.* **1968**, 258.
- (24) Chimichi, S.; Mealli, C. *J. Mol. Struct.* **1992**, *271*, 133.
- (25) Ref 21, p 197f.
- (26) Sohn, Y. S.; Hendrickson, D. N.; Gray, H. B. *J. Am. Chem. Soc.* **1971**, *93*, 3603.
- (27) An extensive discussion on the topic including bibliography can be found in ref 1c, p 319 ff.
- (28) (a) Sakurai, H. *J. Organomet. Chem.* **1980**, *200*, 261. (b) Kumada, M.; Tamao, K. *Adv. Organomet. Chem.* **1968**, *6*, 19.
- (29) Gilman, H.; Atwell, W. H.; Schwebke, G. L. *J. Organomet. Chem.* **1964**, *2*, 369.
- (30) Sakurai, H.; Kumada, M. *Bull. Chem. Soc. Jpn.* **1964**, *37*, 1894.
- (31) Gilman, H.; Atwell, W. H.; Schwebke, G. L. *Chem. Ind.* **1964**, 1063.
- (32) Brook, A. G. *Adv. Organomet. Chem.* **1968**, *7*, 96.
- (33) Brook, A. G.; Anderson, D. G.; Duff, J. M.; Jones, P. F.; MacRae, D. M. *J. Am. Chem. Soc.* **1968**, *90*, 1076.
- (34) Steward, O. W.; Heider, G. L.; Johnson, J. S. *J. Organomet. Chem.* **1979**, *168*, 33.
- (35) Steward, O. W.; Heider, G. L.; Dziedzic, J. E.; Johnson, J. S. *J. Org. Chem.* **1971**, *36*, 3475.
- (36) Tsuji, H.; Terada, M.; Toshimitsu, A.; Tamao, K. *J. Am. Chem. Soc.* **2003**, *125*, 7486.
- (37) Pangborn, A. B.; Giardello, M. A.; Grubbs, R. H.; Rosen, R. K.; Timmers, F. J. *Organometallics* **1996**, *15*, 1518.
- (38) Fleming, I. In *Synthetic Methods of Organometallic and Inorganic Chemistry*, Vol. 2; Auner, N.; Klingebiel, U., Eds.; Thieme: Stuttgart, 1996; p 163.
- (39) Tacke, R.; Wannagat, U. *Monatsh. Chem.* **1975**, *106*, 1005.
- (40) Herberhold, M.; Ayazi, A.; Milius, W.; Wrackmeyer, B. *J. Organomet. Chem.* **2002**, *656*, 71.
- (41) SHELX and SHELXL PC, version 5.03, Bruker AXS, Inc.: Madison, WI, 1994.
- (42) SADABS: Area-Detection Absorption Correction; Bruker AXS Inc.: Madison, WI, 1995.